Letter

Widely tunable two-color x-ray free-electron laser pulses

Eduard Prat,[1,*] Philipp Dijkstal,[1,2] Eugenio Ferrari,[1,†] Romain Ganter,[1] Pavle Juranić,[1] Alexander Malyzhenkov,[1,‡] Sven Reiche,[1] Thomas Schietinger,[1] Guanglei Wang,[1] Andre Al Haddad,[1] Sven Augustin,[1] Christoph Bostedt,[1,3] Gregor Knopp,[1] Jonas Knurr,[1,3] Ana Sofia Morillo-Candas,[1] Zhibin Sun,[1] and Kirsten Schnorr[1]

[1]*Paul Scherrer Institut, CH-5232 Villigen PSI, Switzerland*

[2]*Department of Physics, ETH Zürich, 8092 Zurich, Switzerland*

[3]*École polytechnique fédéral de Lausanne, CH-1015 Lausanne, Switzerland*

(Received 21 February 2022; accepted 4 April 2022; published 2 May 2022)

We demonstrate the generation of widely tunable two-color x-ray free-electron laser (FEL) pulses at SwissFEL. In a split-undulator configuration, each color is produced in a different undulator section, and a chicane between the two sections allows for a variable time separation between the two pulses of up to 500 fs. We show an unprecedented photon energy ratio between the two colors of about three (350 and 915 eV), with each individual pulse having a peak power of a few gigawatts and a duration down to the femtosecond level. Moreover, we demonstrate the reduction of the required undulator length via the optical klystron mechanism and the time-resolved diagnostics of the FEL pulses utilizing the same beam setup as for the pulse generation. The unique combination of widely tunable energy and time separation of the two-color pulse pair offers opportunities to study ultrafast x-ray-induced energy transfer and relaxation processes in physics, chemistry, and biology.

DOI: 10.1103/PhysRevResearch.4.L022025

X-ray free-electron lasers (FELs) are modern research tools that allow the study of matter at atomic time and length scales [1–7]. Scientific interest beyond the standard single-color operation of x-ray FELs is growing, with some experiments requesting an FEL mode with two pulses that are tunable in both photon energy and temporal separation, commonly known as the two-color mode. The availability of such pulses allows following ultrafast x-ray-induced dynamics with unprecedented detail. Previous experiments have demonstrated the high potential of the technique in the XUV and x-ray regime ranging from imaging magnetization dynamics [8], to dissociation of molecules [9], to radiation damage in solids [10]. So far limitations in photon-energy tunability, available delay range, or long pulse duration have limited the range of possible applications.

In this letter, we demonstrate the generation of two-color short FEL pulses with a tunable photon energy ratio up to three, and a time separation of up to 500 fs. With this, we are able to improve upon the tuning range of previous two-color x-ray sources, thus rendering the two-color pump-probe technique available to a much wider class of experiments in physics, chemistry, and biology. Freely tunable x-ray energies enable site-specific excitation and monitoring of subsequent relaxation processes in complex molecular systems. One important example is to study x-ray-induced radiation damage, which is not yet fully understood and crucial for retrieving meaningful data from x-ray FEL experiments. Metal centers in molecules, for instance, coordination compounds, are particularly prone to being the starting point of radiation damage due to their higher absorption cross sections. FEL pulses of temporal durations on the order of inner-shell and core-hole lifetimes, a few to tens of femtoseconds, are necessary for experiments that probe effects linked to these atomic properties. Furthermore, the wide continuous tunability of the temporal delay is as important for obtaining meaningful experimental results.

There are primarily two general approaches to produce two-color x-ray FEL pulses, considering that the FEL radiation wavelength is given by [11] $\lambda = \frac{\lambda_u}{2\gamma^2}(1 + \frac{K^2}{2})$, where λ_u is the period length of the undulator, K is the undulator deflection parameter, and γ is the Lorentz factor of the electron beam. The first type employs two separated ensembles of electrons at different energies (γ) [12–19]. The second type uses two undulator beamlines with different strengths (K) [20–24]. The latter offers better tunability: the temporal separation of the two pulses can be varied in a wide range with a magnetic chicane between the two undulator sections, whereas the wavelength separation can readily be tuned by adjusting the magnetic field of each undulator section. The main drawback of these methods is the need for a long undulator beamline comprising two independent sections.

We will focus on the second type of methods that is often preferred by the user community owing to its larger tunability. There are two variations of this approach, as illustrated in Fig. 1. In the standard option, the same full electron bunch

*eduard.prat@psi.ch

†Present address: Deutsches Elektronen-Synchrotron, D-22607 Hamburg, Germany.

‡Present address: CERN, CH-1211 Geneva 23, Switzerland.

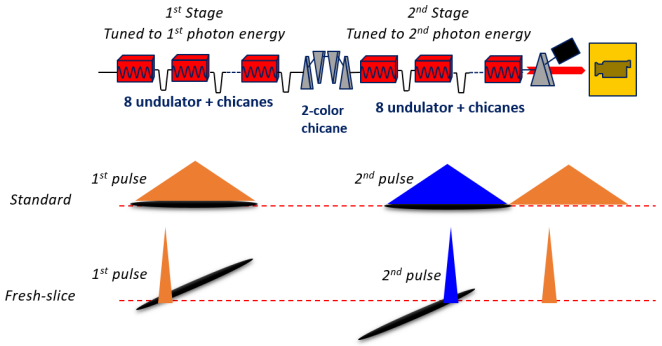

FIG. 1. Schematic layout of the SwissFEL Athos beamline (top) and a cartoon illustrating the generation of tunable two-color pulses in standard (center) and fresh-slice (bottom) configuration.

lases in both undulator sections. In this case, the powers of the two colors are correlated and limited: the increase in energy spread of the electron beam in the first stage due to the FEL process reduces the power of the second pulse. Moreover, this approach does not allow for zero or negative time delay between the two colors (i.e., the pulse produced in the first undulator section arriving at the same time or after the pulse generated in the second section). The minimum delay is the FEL slippage in the first part, which is on the order of a femtosecond for x-rays. This limitation is overcome by the so-called fresh-slice technique whereby only a fraction of the beam is allowed to lase at a time: the bunch tail lases in the first undulator section, the head in the second [23,24]. Such a setup can be achieved by streaking the electron bunch, i.e., imposing a transverse tilt on it (the beam is streaked or transversely tilted if there is a correlation between the transverse and longitudinal coordinates of the electrons). This mode allows driving both pulses into saturation, resulting in a more stable output with higher pulse power. Moreover, it allows for shorter pulses and zero or negative time delays.

We demonstrate the production of tunable two-color x-ray FEL pulses using both the standard and the fresh-slice configuration featuring three advances with respect to previous work: First, we achieve a separation in photon energy corresponding to a factor of about three between the two pulses (915 and 350 eV), to be compared with the 35% level quoted in [22]. Second, we demonstrate a significant reduction of the required undulator length by applying the optical klystron (OK) mechanism (see Ref. [25] and references therein), thus partially compensating for the requirement of an overall longer undulator beamline. Third, we take advantage of the beam tilt needed for the fresh-slice configuration also for the characterization of the time-resolved properties of the x-ray FEL pulses.

The experimental demonstration of this two-color mode was achieved at the Athos soft x-ray beamline at SwissFEL, the x-ray FEL facility in Villigen, Switzerland [26]. The mode was already successfully applied for pilot experiments at the Maloja instrument in the second half of 2021. Figure 1 shows a sketch of Athos. The beamline consists of 16 APPLE-X short undulator modules [27,28] capable of providing variable undulator field and polarization. The undulator modules have a length of 2 m [29], a period of 38 mm, and a maximum undulator deflection parameter K of 3.8. The electron beam energy in the undulator can be adjusted between 2.9 and 3.4 GeV. In combination with an undulator parameter K between 1.2 and 3.8, this corresponds to a photon energy range between 0.26 and 1.68 keV. In our two-color scheme, the first eight modules generate color one, the last eight color two. The large available range in the undulator parameter K allows us to produce two pulses with large photon-energy separation. This setup allows the K parameter to be used as a single knob to select the photon energy for either pump or probe pulse with little impact on the overall machine configuration.

A two-meter magnetic chicane, located in the middle of the undulator beamline, determines the time delay between the two pulses. In fresh-slice mode, the time separation between the two colors can be controlled between a negative time delay corresponding to approximately the FEL pulse duration (typically a few tens of femtoseconds) for zero magnetic field in the chicane and a positive delay of about 500 fs for maximum magnetic field. In the configuration where the full bunch lases, the delay can be controlled between a few femtoseconds for zero magnetic field in the chicane (corresponding to the FEL slippage in the first undulator section) and about 500 fs, corresponding to the maximum magnetic field.

Additional small chicanes of 0.2 m length, installed between every two undulator modules, are used to reduce the saturation length via the OK and to produce FEL pulses with special radiation properties [29]. The chicanes provide a maximum delay of about 8 fs and sufficient precision to control the delay on a subwavelength scale, thus also acting as phase matchers.

The beam tilt for the fresh-slice configuration can be obtained by introducing dispersion at a location where the beam has an energy chirp [30] or by utilizing the transverse wakefields of corrugated or dielectric structures [24]. For the dispersion method, we can generate a horizontal tilt with quadrupole magnets located in the extraction line from the main SwissFEL linac to the Athos undulator. In this location the dispersion amounts to 0.21 m, and the beam energy chirp is about 0.36% (rms). A tilt by wakefields can be obtained with any of the seven corrugated structures that are currently installed upstream of the undulator, with their main purpose to remove the energy chirp of the electron beam. In this work, we applied the dispersion method, with the advantage of producing a mostly linear tilt. The dispersion approach can be readily implemented at any FEL facility without any additional hardware.

In the following, we present the demonstration of the two-color mode in Athos with central photon energies of 915 and 350 eV. The bunch charge was 200 pC, and the electron beam energy was 3.17 GeV. The undulators were set in circular polarization with K values tuned to 1.87 and 3.50, corresponding to the above photon energies. The x-ray pulse energy was measured with a gas-based photon beam intensity monitor [31]. The spectra were measured with a grating spectrometer (with a resolution of approximately 0.5 eV) at the Maloja instrument.

Figure 2 shows the FEL gain curves for the full bunch (without tilt) measured for one undulator section independently at 915 and 350 eV with and without configu-

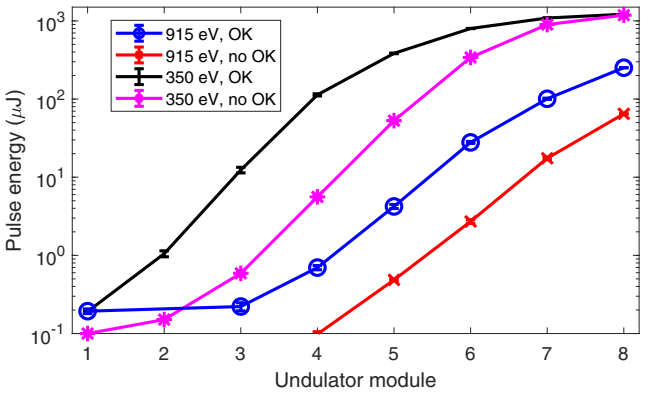

FIG. 2. Measured FEL pulse energy along one undulator section for 915 and 350 eV with and without OK.

ration of the Athos beamline for the OK mode of operation. The 915 eV photons were produced in the first undulator section, the 350 eV ones in the second. Chicane delays and phase shifters were optimized as described in Ref. [25]. For both photon energies, we also optimized the linear taper amplitude of the last undulator modules. For the OK cases, the resulting delay configurations were the following: for the photon energy of 915 eV, the first five chicanes gave delays of 0.83 fs, the sixth a delay of 0.17 fs (the seventh chicane was set to zero delay and acted solely as a phase matcher); for 350 eV photon energy, the first two chicanes were set to delays of 2.33 fs, the third to 1.33 fs, and the fourth to 0.33 fs, with all other chicanes acting as phase matchers only. As shown in Fig. 2, the OK helps to significantly reduce the undulator length required to reach FEL saturation. The OK is indispensable for reducing the longer saturation length at 915 eV. The available eight undulator modules are not enough to reach FEL saturation without OK, instead yielding a final pulse energy of only 65 μJ. With the OK, the pulse energy reaches 250 μJ. For 350 eV, the effect is less relevant, since eight undulator modules are sufficient to reach saturation also without employing the OK: pulse energies above 1 mJ are obtained with and without the OK.

After the gain-curve measurements, taken independently for each photon energy, we produced two colors with the full bunch. The first color, tuned to 915 eV, attained a pulse energy of 250 μJ. The pulse energy of the second color, at 350 eV, was 120 μJ. The reduction of the pulse energy (from above 1 mJ) stems from the spoiling of the electron beam (increase in energy spread) due to lasing in the first undulator section. Higher pulse energy in the second color could be achieved at the expense of pulse energy in the first color, for instance, by detuning the field of one module in the first undulator section.

In a next step we generated the two colors with the fresh-slice configuration. The bunch was horizontally tilted with the dispersion method, using a quadrupole magnet in the Athos extraction line. As a result of the tilt, the center part of the bunch remains on axis in the undulator and therefore lases, while the head and the tail parts of the bunch are off axis and do not lase. An additional correction with dipole magnets can shift the on-axis and lasing fraction of the bunch to the head or the tail. Indeed, corrector magnets before the undulator were

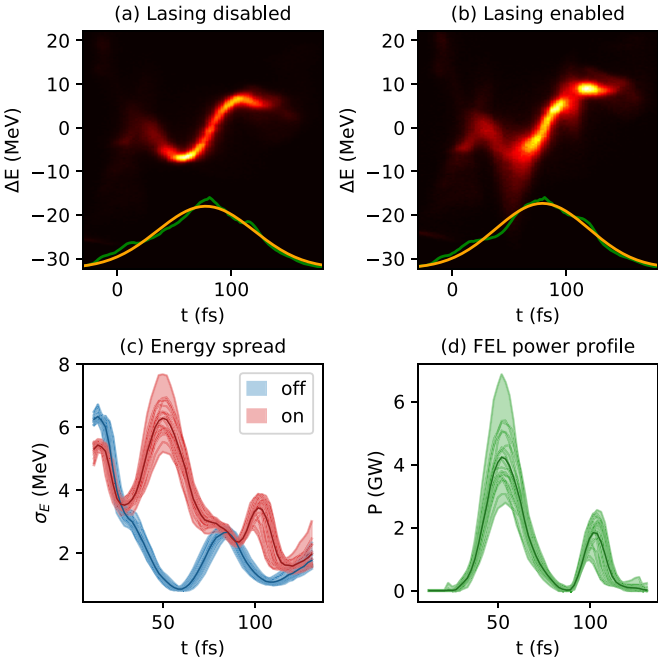

FIG. 3. Top: Longitudinal phase space of the electrons for lasing-off (a) and lasing-on (b) conditions. Green lines are image projections, orange lines show Gaussian fits to these projections. Bottom: Slice energy spread of the electron beam for lasing-off and lasing-on conditions (c) and power profile reconstruction (d). In panels (c) and (d), dark lines are average curves, light lines are individual measurements, and shadings show areas covered by individual measurements.

adjusted to align a slice in the tail in the first undulator half. Likewise magnets in the two-color chicane area were tuned to align a slice in the head in the second undulator part.

The setup and optimization of the fresh-slice configuration requires time-resolved diagnostics. Since a postundulator X-band rf deflector [32] was not commissioned at the time of the measurement, we followed a different approach, which utilizes the tilt also as a temporal diagnostic. The results are shown in Fig. 3. Figures 3(a) and 3(b) display beam images of the reconstructed longitudinal phase space of the electron beam for lasing-off and lasing-on conditions (lasing-off conditions were obtained by slightly detuning the magnetic field of all undulator modules). The beam was measured with a YAG screen at the dump after the undulator beamline, a location with nonzero vertical dispersion. Thus the electron beam energy is obtained from the vertical coordinates and the dispersion value at the screen location (0.23 m for the measurements presented here). The horizontal coordinates are mapped onto a time axis, as explained below. We took 20 images for lasing-off and lasing-on conditions, with the displayed images showing median values. The FEL process causes both an energy loss and an energy spread increase of the lasing electrons. As is evident from Figs. 3(a) and 3(b), there are two distinct parts of the electron beam where energy spread increases when lasing occurs. The right region corresponds to the pulse generated at the first undulator section at 915 eV, with a measured pulse energy of about 30 μJ; the left

part corresponds to the color produced at the second undulator section at 350 eV, with pulse energy around 100 μJ.

The time difference between the two lasing parts was calibrated by scanning the two-color chicane delay when the two pulses were tuned to the same photon energy. For this case, when the pulses arrive at the same time, there is in fact no production of two pulses but an amplification of the first pulse in the so-called multistage amplification mode [33,34]. Thus, the time separation of the two pulses corresponds to the chicane delay giving the maximum output at the second stage. We scanned the magnetic field in the chicane with the two undulator sections tuned to 915 eV to obtain a maximum pulse energy of 110 μJ for a chicane delay of 49.5 fs.

This calibration allows us to convert the horizontal axis to a time axis, provided that the transverse tilt is linear, which is equivalent to assuming that the energy chirp of the electron beam, where the tilt is generated, is also linear [35]. In our case, this assumption is valid for the core of the electron bunch, but it is not fulfilled at the bunch head and tail. In fact, the projection onto the time axis in Figs. 3(a) and 3(b) shows a rather Gaussian current distribution of the electron beam. However, from rf deflector measurements at the hard x-ray beamline and simulations, we expect a current distribution with distinct horn-shaped structures at the head and tail of the bunch. Such horns exhibit high-order time-energy correlations that cannot be captured with this reconstruction method. The energy to time mapping could be improved by calibrating with more points.

The pulse durations given in the following correspond to rms values obtained from Gaussian fits. We quote average values over 20 shots, with errors corresponding to the standard deviation of those shots. In this way we obtain a fitted rms pulse duration of the electron beam of 42.2 ± 0.6 fs. Since the method assumes a linear energy chirp, which is valid only for the core of the bunch, our results should be considered approximate values. The FEL power profile is reconstructed from the difference in slice energy spread of the electron beam between lasing-off and lasing-on conditions following [36–38]. The energy spread is scaled with a factor of $K^{-2/3}$ to account for the different FEL parameter [11] of the two colors [36]. Figure 3(c) displays the energy spread along the electron bunch for lasing-off and lasing-on cases, Fig. 3(d) shows the FEL power profile calculated from these energy spread values. For the right pulse, generated in the first undulator half (915 eV), we reconstruct an estimated peak power of 2.0 ± 0.4 GW and an rms pulse duration of 5.2 ± 0.5 fs, for the left pulse, produced in the second half (350 eV), 4.2 ± 0.9 GW and 9.9 ± 0.5 fs. The time separation between the two pulses of about 50 fs corresponds to the time difference of the lasing slices of the electron beam when the two-color chicane is set to zero field.

If the tilt for the fresh-slice scheme is achieved with wakefields, the temporal diagnostics can be accomplished by the procedure explained in Ref. [38]. This approach does not require the calibration described before, nor the assumption of a linear correlation between energy and time.

Averaged and single-shot spectra, recorded simultaneously for both colors, are shown in Fig. 4 for the full-bunch configuration (equivalent results were obtained for the fresh-slice setup). The spectrometer was aligned in a way as to fit both

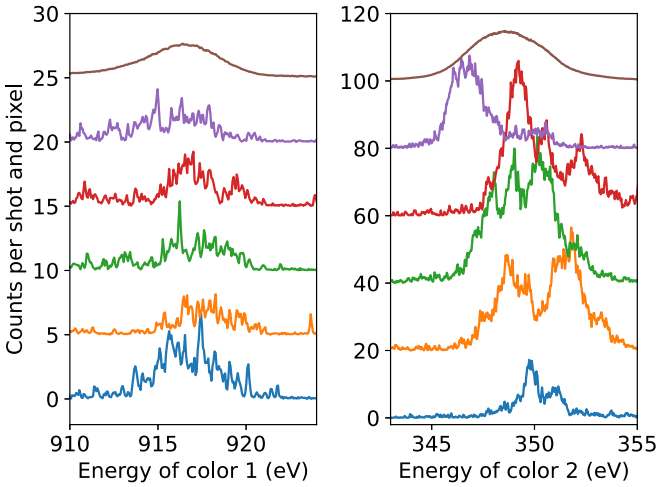

FIG. 4. Averaged (top) and five single-shot spectra of both colors simultaneously recorded.

the second diffraction order of the 915 eV pulse and the fifth diffraction order of the 350 eV pulse on the device for parallel detection of both colors on a single-shot basis.

The two-color x-ray FEL pulses described in this letter have successfully been applied at Athos during two transient-absorption experiments at the Maloja instrument. In a first pump-probe experiment on CO_2, both colors were set to around 530 eV to study the molecular response after core ionization at the oxygen K edge. In the second experiment on N_2O, the pump pulse was tuned to a resonance at the nitrogen K edge around 400 eV, and the initiated dynamics was probed with the second color tuned to the oxygen K edge around 530 eV. In both cases, the photon energies of both colors, as well as the time delay between them, were scanned.

In the future, the potential for large energy separation of the two colors will allow studies of x-ray-induced relaxation dynamics site specifically in a large variety of different molecular systems with absorption edges accessible within the Athos photon energy range. Studying key reactions, such as x-ray-induced charge and energy transfer from a metal center to its environment of light atoms, as typical in coordination complexes, will become possible. In this type of experiments, the first color may be tuned to a metal absorption edge (e.g., $3d$ transition metal L edges) in the energy range between 700 and 1000 eV to excite the system, while the second color may be set to a specific absorption edge of a light element, such as carbon (∼280 eV), nitrogen (∼400 eV) or oxygen (∼530 eV), to probe the initiated dynamics.

To conclude, we have established the generation of widely tunable two-color x-ray FEL pulses at SwissFEL. We have shown an unprecedented photon energy ratio between the two pulses of about three (350 and 915 eV). In addition, we have demonstrated the feasibility of reducing the undulator length required to produce such pulses by use of the OK. Finally, we have shown a full characterization of the time-resolved properties of the electron and photon beams based on the same tilt as is required for the setup of the fresh-slice scheme. This is a straightforward method at no additional cost that can be applied to all special operation modes based on a beam tilt. The two-color pulses have already been exploited in first

pilot experiments of the Maloja instrument at Athos. In the future, this mode will further be capitalized on for site-specific and real-time studies of x-ray-induced relaxation dynamics in heteroatomic systems.

We acknowledge the support of all the technical groups involved in the operation of SwissFEL. The work of P.D. in the context of this project was supported by the Swiss National Science Foundation under Grant No. 200021_175498. The work of A.S.M.-C. was funded by the European Union's Horizon 2020 program under the Marie Skłodowska-Curie grant agreement 884104 (PSI-FELLOW-III-3i). The Maloja instrument received funding from the Swiss National Science Foundation through R'Equip Grant No. 206021_182988.

[1] W. Ackermann, G. Asova, V. Ayvazyan, A. Azima, N. Baboi, J. Bähr, V. Balandin, B. Beutner, A. Brandt, A. Bolzmann, R. Brinkmann, O. I. Brovko, M. Castellano, P. Castro, L. Catani, E. Chiadroni, S. Choroba, A. Cianchi, J. T. Costello, D. Cubaynes *et al.*, Operation of a free-electron laser from the extreme ultraviolet to the water window, Nat. Photonics **1**, 336 (2007).

[2] P. Emma, R. Akre, J. Arthur, R. Bionta, C. Bostedt, J. Bozek, A. Brachmann, P. Bucksbaum, R. Coffee, F.-J. Decker, Y. Ding, D. Dowell, S. Edstrom, A. Fisher, J. Frisch, S. Gilevich, J. Hastings, G. Hays, P. Hering, Z. Huang *et al.*, First lasing and operation of an ångstrom-wavelength free-electron laser, Nat. Photonics **4**, 641 (2010).

[3] T. Ishikawa, H. Aoyagi, T. Asaka, Y. Asano, N. Azumi, T. Bizen, H. Ego, K. Fukami, T. Fukui, Y. Furukawa, S. Goto, H. Hanaki, T. Hara, T. Hasegawa, T. Hatsui, A. Higashiya, T. Hirono, N. Hosoda, M. Ishii, T. Inagaki *et al.*, A compact X-ray free-electron laser emitting in the sub-ångström region, Nat. Photonics **6**, 540 (2012).

[4] E. Allaria, D. Castronovo, P. Cinquegrana, P. Craievich, M. D. Forno, M. B. Danailov, G. D'Auria, A. Demidovich, G. D. Ninno, S. D. Mitri, B. Diviacco, W. M. Fawley, M. Ferianis, E. Ferrari, L. Froehlich, G. Gaio, D. Gauthier, L. Giannessi, R. Ivanov, B. Mahieu *et al.*, Two-stage seeded soft-x-ray free-electron laser, Nat. Photonics **7**, 913 (2013).

[5] H.-S. Kang, C.-K. Min, H. Heo, C. Kim, H. Yang, G. Kim, I. Nam, S. Y. Baek, H.-J. Choi, G. Mun, B. R. Park, Y. J. Suh, D. C. Shin, J. Hu, J. Hong, S. Jung, S.-H. Kim, K. Kim, D. Na, S. S. Park *et al.*, Hard X-ray free-electron laser with femtosecond-scale timing jitter, Nat. Photonics **11**, 708 (2017).

[6] W. Decking, S. Abeghyan, P. Abramian, A. Abramsky, A. Aguirre, C. Albrecht, P. Alou, M. Altarelli, P. Altmann, K. Amyan, V. Anashin, E. Apostolov, K. Appel, D. Auguste, V. Ayvazyan, S. Baark, F. Babies, N. Baboi, P. Bak, V. Balandin *et al.*, A MHz-repetition-rate hard x-ray free-electron laser driven by a superconducting linear accelerator, Nat. Photonics **14**, 391 (2020).

[7] E. Prat, R. Abela, M. Aiba, A. Alarcon, J. Alex, Y. Arbelo, C. Arrell, V. Arsov, C. Bacellar, C. Beard, P. Beaud, S. Bettoni, R. Biffiger, M. Bopp, H.-H. Braun, M. Calvi, A. Cassar, T. Celcer, M. Chergui, P. Chevtsov *et al.*, A compact and cost-effective hard x-ray free-electron laser driven by a high-brightness and low-energy electron beam, Nat. Photonics **14**, 748 (2020).

[8] E. Ferrari, C. Spezzani, F. Fortuna, R. Delaunay, F. Vidal, I. Nikolov, P. Cinquegrana, B. Diviacco, D. Gauthier, G. Penco, P. R. Ribič, E. Roussel, M. Trovò, J.-B. Moussy, T. Pincelli, L. Lounis, M. Manfredda, E. Pedersoli, F. Capotondi, C. Svetina *et al.*, Widely tunable two-colour seeded free-electron laser source for resonant-pump resonant-probe magnetic scattering, Nat. Commun. **7**, 10343 (2016).

[9] A. Picón, C. S. Lehmann, C. Bostedt, A. Rudenko, A. Marinelli, T. Osipov, D. Rolles, N. Berrah, C. Bomme, M. Bucher, G. Doumy, B. Erk, K. R. Ferguson, T. Gorkhover, P. J. Ho, E. P. Kanter, B. Krässig, J. Krzywinski, A. A. Lutman, A. M. March *et al.*, Hetero-site-specific x-ray pump-probe spectroscopy for femtosecond intramolecular dynamics, Nat. Commun. **7**, 11652 (2016).

[10] I. Inoue, Y. Inubushi, T. Sato, K. Tono, T. Katayama, T. Kameshima, K. Ogawa, T. Togashi, S. Owada, Y. Amemiya, T. Tanaka, T. Hara, and M. Yabashi, Observation of femtosecond X-ray interactions with matter using an X-ray–X-ray pump–probe scheme, Proc. Natl. Acad. Sci. USA **113**, 1492 (2016).

[11] R. Bonifacio, C. Pellegrini, and L. M. Narducci, Collective instabilities and high-gain regime in a free electron laser, Opt. Commun. **50**, 373 (1984).

[12] A. Marinelli, D. Ratner, A. Lutman, J. Turner, J. Welch, F.-J. Decker, H. Loos, C. Behrens, S. Gilevich, A. Miahnahri, S. Vetter, T. Maxwell, Y. Ding, R. Coffee, S. Wakatsuki, and Z. Huang, High-intensity double-pulse X-ray free-electron laser, Nat. Commun. **6**, 6369 (2015).

[13] Y. Ding, C. Behrens, R. Coffee, F.-J. Decker, P. Emma, C. Field, W. Helml, Z. Huang, P. Krejcik, J. Krzywinski, H. Loos, A. Lutman, A. Marinelli, T. J. Maxwell, and J. Turner, Generating femtosecond X-ray pulses using an emittance-spoiling foil in free-electron lasers, Appl. Phys. Lett. **107**, 191104 (2015).

[14] A. Marinelli, R. Coffee, S. Vetter, P. Hering, G. N. West, S. Gilevich, A. A. Lutman, S. Li, T. J. Maxwell, J. Galayda, A. Fry, and Z. Huang, Optical Shaping of X-Ray Free-Electron Lasers, Phys. Rev. Lett. **116**, 254801 (2016).

[15] F.-J. Decker, K. L. F. Bane, W. S. Colocho, A. A. Lutman, and J. C. Sheppard, Recent developments and plans for two bunch operation with up to 1 μs separation at LCLS, in *Proceeding of 38th International Free Electron Laser conference (FEL'17), Santa Fe, USA*, paper TUP023 (JACoW, Geneva, 2018), pp. 288–291.

[16] P. Dijkstal, A. Malyzhenkov, S. Reiche, and E. Prat, Demonstration of two-color x-ray free-electron laser pulses with a sextupole magnet, Phys. Rev. Accel. Beams **23**, 030703 (2020).

[17] A. Malyzhenkov, Y. P. Arbelo, P. Craievich, P. Dijkstal, E. Ferrari, S. Reiche, T. Schietinger, P. Juranić, and E. Prat, Single- and two-color attosecond hard x-ray free-electron laser pulses with nonlinear compression, Phys. Rev. Research **2**, 042018(R) (2020).

[18] S. Bettoni, P. Craievich, A. Dax, R. Ganter, M. Guetg, M. Huppert, F. Marcellini, R. N. Pestana, S. Reiche, E. Prat, A. Trisorio, C. Vicario, and A. Lutman, Experimental demonstration of two-color x-ray free-electron-laser pulses via wakefield excitation, Phys. Rev. Accel. Beams **24**, 08801 (2021).

[19] C. Vicario, S. Bettoni, A. Lutman, A. Dax, M. Huppert, and A. Trisorio, Two-color x-ray free-electron laser by photocathode laser emittance spoiler, Phys. Rev. Accel. Beams **24**, 060703 (2021).

[20] D. A. Jaroszynski, R. Prazeres, F. Glotin, and J. M. Ortega, Two-Color Free-Electron Laser Operation, Phys. Rev. Lett. **72**, 2387 (1994).

[21] A. A. Lutman, R. Coffee, Y. Ding, Z. Huang, J. Krzywinski, T. Maxwell, M. Messerschmidt, and H.-D. Nuhn, Experimental Demonstration of Femtosecond Two-Color X-Ray Free-Electron Lasers, Phys. Rev. Lett. **110**, 134801 (2013).

[22] T. Hara, Y. Inubushi, T. Katayama, T. Sato, H. Tanaka, T. Tanaka, T. Togashi, K. Togawa, K. Tono, M. Yabashi, and T. Ishikawa, Two-colour hard X-ray free-electron laser with wide tunability, Nat. Commun. **4**, 2919 (2013).

[23] S. Reiche and E. Prat, Two-color operation of a free-electron laser with a tilted beam, J. Synchrotron Radiat. **23**, 869 (2016).

[24] A. A. Lutman, T. J. Maxwell, J. P. MacArthur, M. W. Guetg, N. Berrah, R. N. Coffee, Y. Ding, Z. Huang, A. Marinelli, S. Moeller, and J. C. U. Zemella, Fresh-slice multicolour X-ray free-electron lasers, Nat. Photonics **10**, 745 (2016).

[25] E. Prat, E. Ferrari, M. Calvi, R. Ganter, S. Reiche, and T. Schmidt, Demonstration of a compact x-ray free-electron laser using the optical klystron effect, Appl. Phys. Lett. **119**, 151102 (2021).

[26] R. Abela, A. Alarcon, J. Alex, C. Arrell, V. Arsov, S. Bettoni, M. Bopp, C. Bostedt, H.-H. Braun, M. Calvi, T. Celcer, P. Craievich, A. Dax, P. Dijkstal, S. Dordevic, E. Ferrari, U. Flechsig, R. Follath, F. Frei, N. Gaiffi *et al.*, The SwissFEL soft x-ray free-electron laser beamline: Athos, J. Synchrotron Rad. **26**, 1073 (2019).

[27] T. Schmidt and M. Calvi, APPLE x undulator for the SwissFEL soft x-ray beamline athos, Synchrotron Radiat. News **31**, 35 (2018).

[28] X. Liang, M. Calvi, M.-E. Couprie, R. Ganter, C. Kittel, N. Sammut, T. Schmidt, M. Valléau, and K. Zhang, Analysis of the first magnetic results of the PSI APPLE X undulators in elliptical polarisation, Nucl. Instrum. Methods Phys. Res. A **987**, 164741 (2021).

[29] E. Prat, M. Calvi, R. Ganter, S. Reiche, T. Schietinger, and T. Schmidt, Undulator beamline optimization with integrated chicanes for X-ray free-electron-laser facilities, J. Synchrotron Radiat. **23**, 861 (2016).

[30] M. W. Guetg, A. A. Lutman, Y. Ding, T. J. Maxwell, and Z. Huang, Dispersion-Based Fresh-Slice Scheme for Free-Electron Lasers, Phys. Rev. Lett. **120**, 264802 (2018).

[31] A. A. Sorokin, Y. Bican, S. Bonfigt, M. Brachmanski, M. Braune, U. F. Jastrow, A. Gottwald, H. Kaser, M. Richter, and K. Tiedtke, An x-ray gas monitor for free-electron lasers, J. Synchrotron Rad. **26**, 1092 (2019).

[32] P. Craievich, M. Bopp, H.-H. Braun, A. Citterio, R. Fortunati, R. Ganter, T. Kleeb, F. Marcellini, M. Pedrozzi, E. Prat, S. Reiche, K. Rolli, R. Sieber, A. Grudiev, W. Millar, N. Catalan-Lasheras, G. McMonagle, S. Pitman, V. del Pozo Romano, K. Szypula *et al.*, Novel *X*-band transverse deflection structure with variable polarization, Phys. Rev. Accel. Beams **23**, 112001 (2020).

[33] E. Prat, F. Löhl, and S. Reiche, Efficient generation of short and high-power x-ray free-electron-laser pulses based on superradiance with a transversely tilted beam, Phys. Rev. ST Accel. Beams **18**, 100701 (2015).

[34] A. A. Lutman, M. W. Guetg, T. J. Maxwell, J. P. MacArthur, Y. Ding, C. Emma, J. Krzywinski, A. Marinelli, and Z. Huang, High-Power Femtosecond Soft X Rays from Fresh-Slice Multistage Free-Electron Lasers, Phys. Rev. Lett. **120**, 264801 (2018).

[35] E. Prat and M. Aiba, General and efficient dispersion-based measurement of beam slice parameters, Phys. Rev. ST Accel. Beams **17**, 032801 (2014).

[36] Z. Huang, K. Bane, Y. Cai, A. Chao, R. Hettel, and C. Pellegrini, Steady-state analysis of short-wavelength, high-gain FELs in a large storage ring, Nucl. Instrum. Methods Phys. Res. A **593**, 120 (2008).

[37] C. Behrens, F.-J. Decker, Y. Ding, V. A. Dolgashev, J. Frisch, Z. Huang, P. Krejcik, H. Loos, A. Lutman, T. J. Maxwell, J. Turner, J. Wang, M.-H. Wang, J. Welch, and J. Wu, Few-femtosecond time-resolved measurements of x-ray free-electron lasers, Nat. Commun. **5**, 3762 (2014).

[38] P. Dijkstal, A. Malyzhenkov, P. Craievich, E. Ferrari, R. Ganter, S. Reiche, T. Schietinger, P. Juranić, and E. Prat, Self-synchronized and cost-effective time-resolved measurements at x-ray free-electron lasers with femtosecond resolution, Phys. Rev. Research **4**, 013017 (2022).